nature materials

SUPPLEMENTARY INFORMATION

DOI: 10.1038/NMAT3990

A Stable Three-dimensional Topological Dirac Semimetal Cd_3As_2

Z. K. Liu, J. Jiang, B. Zhou, Z. J. Wang, Y. Zhang, H. M. Weng, D. Prabhakaran,
S. -K. Mo, H. Peng, P. Dudin, T. Kim, M. Hoesch, Z. Fang, X. Dai,
Z. X. Shen, D. L. Feng, Z. Hussain, and Y. L. Chen

This file includes:

DOI: 10.1038/NMAT3990

SI A: Experiment geometry of the ARPES measurement:

The measured ARPES signal intensity (I_0) is affected by the photoemission matrix element: $I_0 \propto \left|\langle \phi_f^k | \vec{\varepsilon} \cdot \vec{x} | \phi_i^k \rangle\right|^2$, where ϕ_i^k and ϕ_i^k are the wavefunctions for the initial and final states. $\vec{\varepsilon}$ is the unit vector along the polarization vector $\hat{E}$ and $\vec{x}$ is the position operator. Thus different photon polarization and measurement geometries can result in enhanced or suppressed ARPES signal intensity for initial states (bands) with different symmetries [S1].

We performed ARPES measurements with different light polarization and measurement geometries. The measurement geometries for the plots in the main text Fig. 2a, b are shown in Fig. S1 below. The photon polarization used in Fig. 2a and Fig. 2b is $\hat{E}_{\mathrm{mix}}$ (mixture of polarization) and $\hat{E}_{\mathrm{s}}$ (perpendicular to the incident plane and parallel to the $\bar{\mathrm{M}} - \bar{\Gamma} - \bar{\mathrm{M}}$ direction and the analyzer slit), respectively. To enhance the photoemission intensity of the 3D Dirac band and suppress the other parabolic band in Fig. 2a, the $\hat{E}_{\mathrm{s}}$ polarization was used.

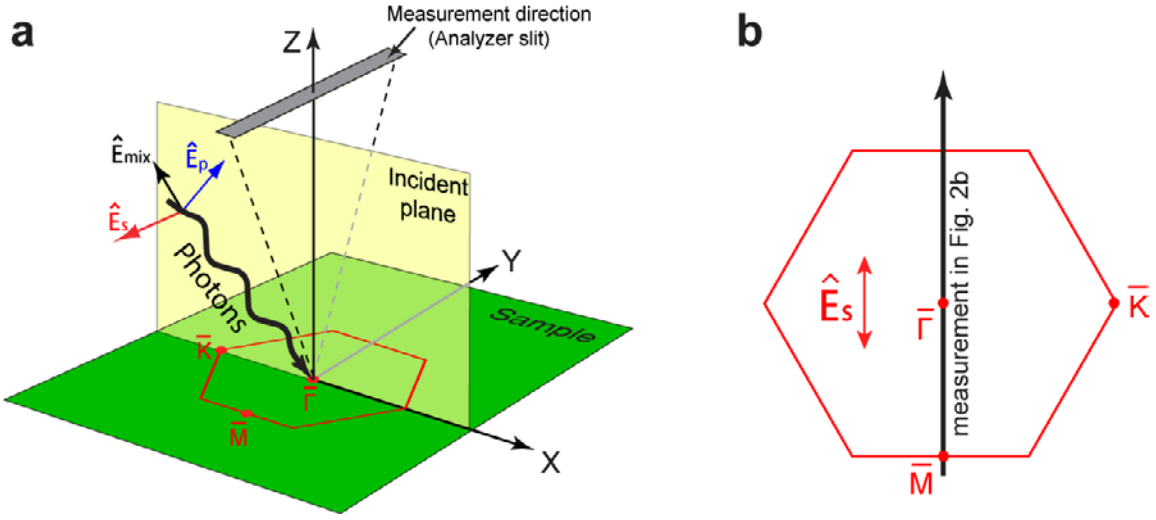

Fig. S1| Illustration of the experiment geometry. (a) Experimental setup with mixed ($\hat{E}_{\mathrm{mix}}$), perpendicular ($\hat{E}_{\mathrm{s}}$) and in-plane ($\hat{E}_{\mathrm{p}}$) polarizations of photons (with respect to the incident plane), indicated by the black, red and blue arrows, respectively. The red hexagon represents the Brillouin Zone (BZ) orientation, and the gray bar on top shows the direction of the analyzer slits where measurements are performed. The measurements in Fig. 2a and 2b of the main text were performed with $\hat{E}_{\mathrm{mix}}$ and $\hat{E}_{\mathrm{s}}$,

respectively. (b) Sketch of the measurement geometry in the projected two-dimensional BZ for the main text Fig. 2b.

SI B: Photon energy dependent ARPES measurements

B1: k_z-momentum determination:

ARPES measurement can determine the in-plane momentum ($k_{//}$, parallel to the sample surface) of electrons in solids naturally by the momentum conservation of photoelectrons [S2]; while determining the out-of-plane momentum component (k_z) is less straightforward - which requires a set of ARPES measurements performed under different photon energies [S1, S3].

Based on the nearly free-electron final state approximation with a potential parameter V_0 (also known as the inner potential) describing the energy difference from the bottom of the final state band to the vacuum level, we can derive the k_z as [S1, S3]:

$$k_z = \sqrt{\frac{2m_e^*}{\hbar^2}(E_k + V_0) - k_{\parallel}^2} = \sqrt{\frac{2m_e^*}{\hbar^2}(E_k + V_0) - \frac{2m_e E_k}{\hbar^2}\sin^2\theta}$$

where θ is the emission angle, m_e* is the effective mass of electrons in the final bulk states [S4, S5] and E_k is the kinetic energy of the emitted free electrons, which satisfies:

$$E_k = h\upsilon - w - E_B$$

where $h\upsilon$ is the photon energy, w is the work function of the sample and E_B is the electron binding energy .

As V_0 is material dependent, we performed energy dependent ARPES by using a broad range of photon energies to cover sufficient k_z–span - ideally more than the k_z size of one BZ - and used the high symmetry points in the BZ to identify the exact value of k_z.

DOI: 10.1038/NMAT3990

B2: Complete band and Fermi-surface mapping throughout the entire 3D Brillouin zone

Part I: Determine k_z momentum by wide range photon energy coverage:

With the broad photon energy range of Beamline I05 at Diamond Light Source, we performed photon energy dependent ARPES to obtain the complete electronic structures of Cd_3As_2 [band dispersions and Fermi-surfaces (FS)] throughout an entire 3D BZ.

We scanned the photon energy from 60eV to 225eV in the ARPES measurements (which covered ~2 BZ size along the k_z direction) (see Fig. S2 below). The high symmetry points (e.g. Γ and Dirac points) in both BZs allow us to determine the exact k_z locations as discussed above in SI part B1 (V_0 =10.6eV).

From Fig. S2, we can also determine that the Dirac points locate at k_x=k_y=*0* and k_z= ±0.16 $Å^{-1}$ = ±*0.*18π/c; which is close to our calculation value : k_z= ± 0.12$Å^{-1}$ = ±0.14 π/c (see SI part D below).

After determining the k_z value, together with the in-plane momentum k_x, k_y (Fig. S1) and electron energy E, we obtained the full electronic structure of Cd_3As_2 (with all four parameters*:* k_x, k_y, k_z, and E) around the Dirac points, as illustrated in Fig. 2-4 of the main text.

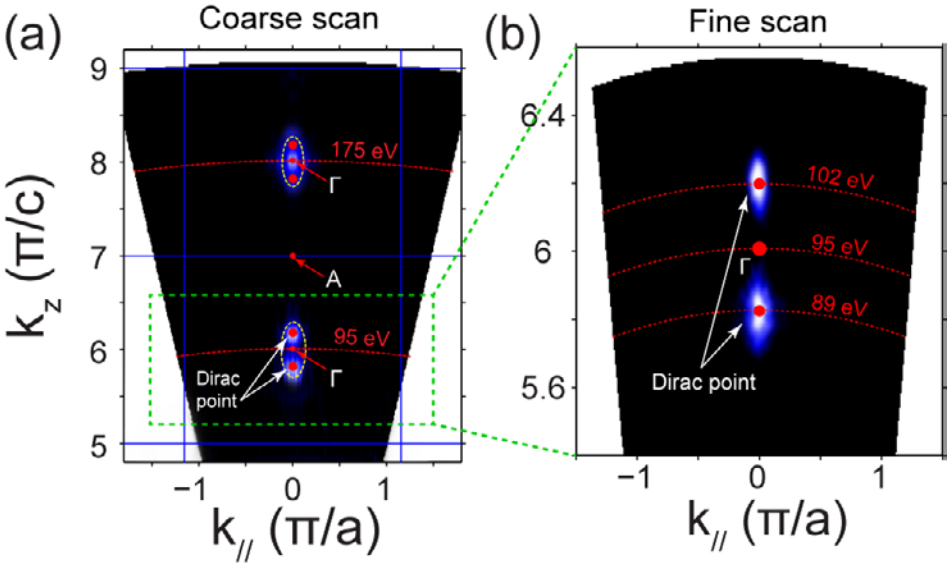

Fig. S2| Determination of k_z momentum by photon energy dependent ARPES. (a) Fermi surface (FS) map of ARPES spectra from a broad scan of photon energy (60~225eV with 5eV step) showing the coverage of 2 BZs. Overlaid blue rectangles represent the vertical BZs of Cd_3As_2 with the high symmetry points indicated. Red dotted curves represent the measurements that cut through the Γ points, with the corresponding photon energies indicated. (b) Zoom-in measurement around the Γ point with finer k_z steps

(75 ~ 115 eV photon energy with 1 eV step). Two Dirac points can be clearly resolved at 89 eV and 102 eV, respectively.

Part II: Estimation of the k_z resolution:

After reconstructing the full 3D electronic structure above, we can study the band dispersion along the k_z direction (see Fig. S3 below) and determine the k_z resolution (δk_z) of our experiment.

The photoemission intensity along the k_z direction in an ARPES measurement $I(k_z, E)$ can be written as the convolution of the true ARPES signal and the (2D) resolution function $R(\delta k_z, \delta E)$:

$$I(k_z, E) \propto [|M_{f,i}^k|^2 \cdot A(k_z, E) \cdot f(E)] * R(\delta k_z, \delta E) \quad (1)$$

where k_z is the electron momentum, E is the electron energy (with respect to the Fermi level); $|M_{f,i}^k|$ is the one-electron photoemission matrix element; $A(k, E)$ is the one-particle spectral function and $f(E)$ is the Fermi-Dirac function $f(E) = (e^{\frac{E}{k_B T}} + 1)^{-1}$ which accounts for the fact that direct photoemission probes only the occupied electronic states. $R(\delta k, \delta E)$ is the 2D momentum and energy resolution function, which typically has the Gaussian form: $e^{\left\{-\frac{1}{\sqrt{2}}\cdot\left(\left(\frac{K_Z}{\delta K_Z}\right)^2+\left(\frac{E}{\delta E}\right)^2\right)\right\}}$ and should be convolved to give the final experimental spectra.

The k_z dispersion of the bulk Dirac band from our measurements is shown in Fig. S3a, which can be fitted by equation (1) (the fitting parameters and the results are explained in the caption of Fig. S3). The fitted results and the comparison to the original spectra are plotted in Fig. S3b. From the fitting, we can obtain the k_z resolution ($\delta k_z = 0.035 \text{Å}^{-1}$) of our experiments and the Dirac fermion velocity along the k_z direction (V_z = 2.1 eV•Å).

Compared to the large k_z size of a full BZ ($k_z^{BZ} = 2\frac{\pi}{c}$) due to the small lattice constant c (3.66 Å), the $\delta k_z = 0.035 \text{Å}^{-1} = 0.02\, k_z^{BZ}$ is much smaller, i.e. $\delta k_z \ll k_z^{BZ}$. Thus in this case, we can faithfully determine the band structures along the k_z direction [S6].

Finally, from the fitting, the Dirac fermion velocity along k_z is determined to be $V_z \approx$ 2.16eV•Å (or 3.27 $\times 10^5$ m/s), which is much smaller than V_x and V_y ($V_z = 0.25 V_y$), in consistent with the large anisotropy result from our calculation ($V_z = 0.26 V_y$, see SI part D below).

DOI: 10.1038/NMAT3990

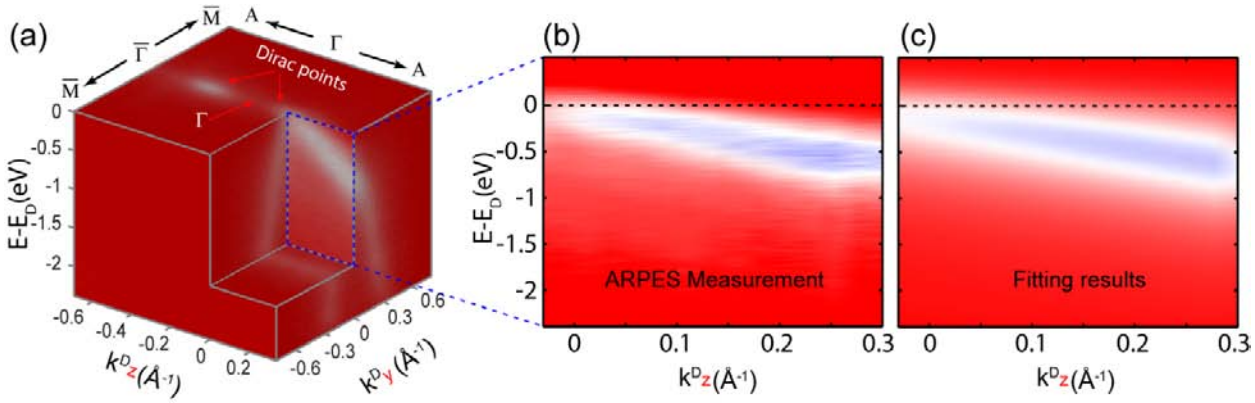

Fig. S3| Estimation of the k_z resolution δk_z. (a) 3D plot of the ARPES spectra intensity showing the linear dispersion along k_y and k_z directions. (b) Band dispersion along the k_z direction. The intensity change with k_z is due to the matrix element ($|M^k_{f,i}|^2$) effect. (c) The fitted k_z dispersions in panel (b) by equation *(1)* showing good agreement. In the fitting process, we used a 2nd order polynomial to represent the matrix element variation along the k_z direction: $|M^k_{f,i}|^2 = 1 + M1 \cdot k_z + M2 \cdot {k_z}^2$, where M1 and M2 are two fitting parameters; we use the bare spectra function $A(k_z, E) = \delta(E - V_z\, k_z)$ to represent the bulk Dirac band dispersion $E = V_z\, k_z$, in which V_z is a fitting parameter; experiment temperature T=80K was used in the Fermi-Dirac function. For the resolution function $R(\delta k_z, \delta E)$, the δE is the total experiment energy resolution fixed to be ~0.03eV (see discussion in text), and the δk_z is the fitting parameter representing the k_z resolution.

SI C: Fitting of the 3D Dirac band

For a 3D Dirac cone, the extracted band dispersion in each (2D) ARPES measurement is either linear or hyperbolic (main text Fig. 4a-c), depending on whether the measurement cuts through the 3D Dirac point.

As the linear dispersions in Fig. 2b, 2d(iv), Fig. 3b, e, f and Fig. 4a(i)-c(i) of the main text are obvious, in Fig. S4 (c, d) we compare the fittings of a hyperbola and a parabola from a typical dispersion away from the Dirac point (k^Dz=0.45 Å^{-1}). Clearly, the fitting to the hyperbola (Fig. S4c) is excellent while in contrast, the fitting to a parabola (Fig. S4d) shows clear discrepancy.

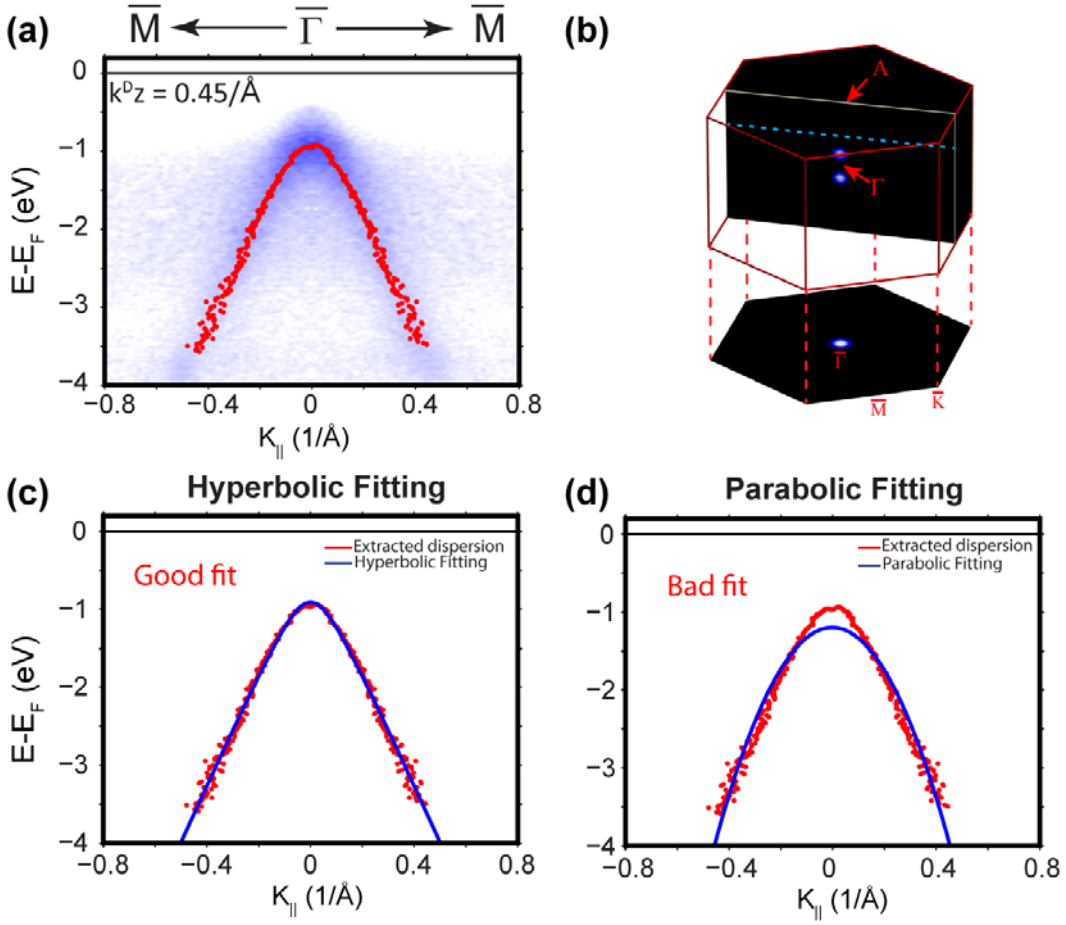

Fig. S4| Fitting the dispersion. (a) ARPES intensity plot of the measurement along the $\bar{M}$- $\bar{\Gamma}$-$\bar{M}$ direction at k^Dz=0.45 Å^{-1} (the measurement position is indicated by the blue dashed line marked in the 3D BZ in (b). The red dots indicate the dispersion extracted from MDC and EDC analysis. (c, d) Fitting of the extracted dispersion (red dotted curves) in (a) with a hyperbolic (c) and a parabolic (d) curve, respectively. Obviously, the fitting in (c) is excellent while that in (d) shows clear discrepancy.

DOI: 10.1038/NMAT3990

SI D: *Ab initio* calculations of the band structures

The details of the method of our *ab initio* calculations have been summarized in the "methods" section of the main text. The calculated band structure is plotted in Fig. S5(a); and a zoom-in plot of the dispersion along the k_z direction is shown in Fig. S5(b). The calculated positions of the two 3D Dirac points are: (k_x, k_y, k_z) = (0, 0, ±0.12Å^{-1})); and the calculated Fermi velocity (V_x, V_y, V_z) = (5 eV•Å^{-1}, 5.8 eV•Å, 1.5 eV•Å^{-1}), respectively, also showing large anisotropy between the k_z and k_x/k_y directions (V_z=0.26V_y), similar to what we got from experiments (V_x=0.25V_y).

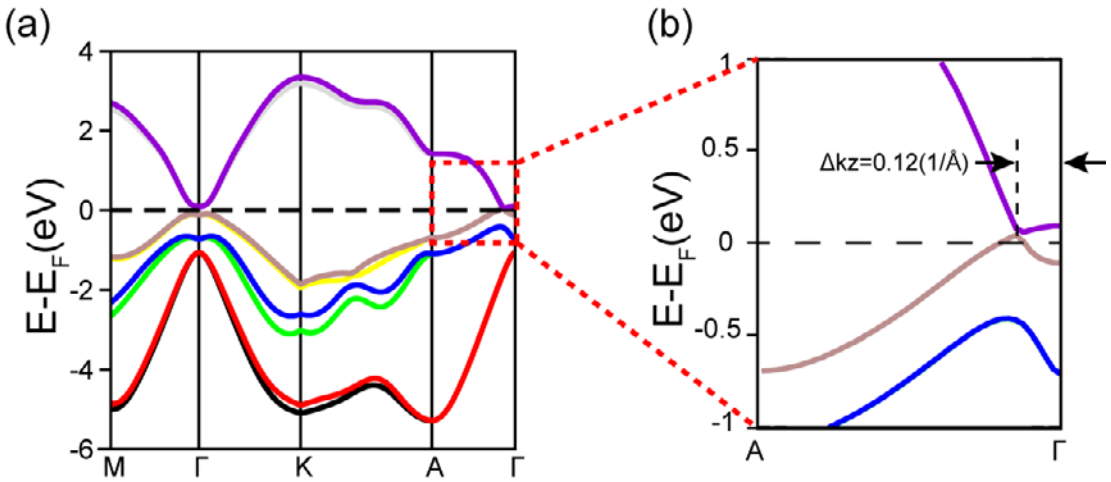

Fig. S5| Band structure of Cd_3As_2 by *ab initio* calculation (a) Band dispersions by *ab initio* calculation using the unit cell in main text Fig.1a. Different colors represent different electronic bands. (b) Zoom-in plot of the dispersion along the Γ-A line where 3D Dirac point is located. The calculated positions of the 3D Dirac points along the [111] direction are $k_z = \pm 0.12$ Å^{-1}.

References:

S1. Damascelli, A., Hussain, Z. & Shen, Z.-X. Angle-resolved photoemission studies of the cuprate superconductors. *Rev. Mod. Phys.,* **75**, 473-541 (2003).

S2. Chen, Y. Studies on the electronic structures of three-dimensional topological insulators by angle resolved photoemission spectroscopy. *Front. Phys*. **7**, 175-192 (2012).

S3. Damascelli, A. Probing the Electronic Structure of Complex Systems by ARPES. *Phys. Script.*, **2004**, 61-74(2004)

S4. Hüfner, S. *Photoelectron Spectroscopy: Principles and Applications*. Springer, 2003

S5. Samsavar, A., Miller, T. & Chiang, T. –C. Photoemission study of the final band in Ag(111). *J. Phys.: Condens. Matter*, **2**, 1141(1990)

S6. Strocov, V. N. Intrinsic accuracy in 3-dimensional photoemission band mapping. *J. Electron. Spectrosc. Relat. Phenom.* **130**, 65-78 (2003).